Asymptotic Prethermalization in Periodically Driven Classical Spin Chains

Nimish Sharma Anshul Maheshwari

BITS Pilani, Pilani Campus

May 3, 2025

Submitted to: Prof. Jayendra Nath Bandopadhyay

Contents

1 Introduction and Key Concepts **2**
- 1.1 Floquet Engineering . . . 2
- 1.2 Periodic Driving . . . 3
- 1.3 Heating and Thermalization . . . 3
- 1.4 Prethermalization . . . 4

2 Model **5**

3 Equations of motion **6**
- 3.1 First Half-Period: Rotation About the z-Axis (Map τ_1) . . . 6
- 3.2 Second Half-Period: Rotation About the x-Axis (Map τ_2) . . . 7
- 3.3 Summary of evolution over the entire period . . . 8

4 Modified Hamiltonian **9**
- 4.1 Equations of Motion for the Modified Hamiltonian . . . 9
  - 4.1.1 First Half–Period: Rotation about z-Axis . . . 9
  - 4.1.2 Second Half–Period: Rotation about x-Axis . . . 10
  - 4.1.3 Summary of Evolution over One Full Cycle . . . 10

5 Methodology **11**
- 5.1 Ground-State Preparation at High Drive Frequencies . . . 11
  - 5.1.1 Linear Hamiltonian . . . 11
  - 5.1.2 Quadratic Hamiltonian . . . 11
- 5.2 Noise Realizations and Ensemble Averages . . . 12
  - 5.2.1 Four Dynamical Stages of Evolution . . . 12
- 5.3 Energy Observables: $\langle Q(lT)\rangle$ . . . 13
- 5.4 Noise-Averaged Expected Energy vs. Driving Cycles . . . 13

6 Simulation and Code **15**
- 6.1 Explanation of the C++ Simulation Code for the Linear Hamiltonian . . . 15
- 6.2 Explanation of the C++ Simulation Code for the Quadratic Hamiltonian 17

7 Results and Discussion **18**
- 7.1 Linear Hamiltonian Results . . . 18
- 7.2 Quadratic Hamiltonian Results . . . 19

8 Scope for Advancement **20**
- 8.1 Expected Behavior During Thermalization . . . 20

Chapter 1

Introduction and Key Concepts

1.1 Floquet Engineering

The cornerstone of Floquet theory in physics is Floquet's theorem. However, the theorem applies to linear ordinary differential equations, and hence its consequences become invalid for systems obeying nonlinear dynamics. On the other hand, chaos and thermalization are intimately tied to the nonlinearities in the Hamilton equations of motion. Therefore, finding effective descriptions for classical periodically-driven many-body systems is a challenging and difficult problem, and there might not exist a simple universal solution.

The starting point in Floquet theory is the assumption that the Floquet Hamiltonian can be expanded in a Taylor series in the inverse frequency:

$$H_F \;=\; \sum_{n=0}^{\infty} H_F^{(n)}, \quad H_F^{(n)} \sim \mathcal{O}(\Omega^{-n}), \quad H_F^{(0+\cdots+m)} \;=\; \sum_{n=0}^{m} H_F^{(n)}.$$

Let us apply the Magnus expansion—a variant of the inverse-frequency expansion—to the step-driven spin chain. Writing the time-dependent Hamiltonian as

$$\hat{H}(t) = \begin{cases} \widehat{A}, & t \in [0, T/2) \bmod T, \\ \widehat{B}, & t \in [T/2, T) \bmod T, \end{cases}$$

where

$$\widehat{A} \;=\; \sum_{j=1}^{N} \Big(J\, \hat{S}_j^z \hat{S}_{j+1}^z \;+\; h\, \hat{S}_j^z \Big), \quad \widehat{B} \;=\; \sum_{j=1}^{N} g\, \hat{S}_j^x,$$

the one-cycle evolution operator becomes

$$U(T,0) \;=\; \exp\Big(-i \hat{H}_F T\Big) \;=\; \exp\Big(-i\, \widehat{B}\, \tfrac{T}{2}\Big)\, \exp\Big(-i\, \widehat{A}\, \tfrac{T}{2}\Big).$$

For this setup, applying the Magnus expansion is equivalent to using the Baker–Campbell–Hausdorff formula. To third order in the inverse frequency (or period T), the Floquet Hamiltonian terms are:

$$\widehat{H}_{\text{ave}} = \widehat{H}_F^{(0)} = \tfrac{1}{2}\Big(\widehat{A} + \widehat{B}\Big),$$

$$\widehat{H}_F^{(1)} = \tfrac{T}{8}\Big[\widehat{B},\, \widehat{A}\Big],$$

$$\widehat{H}_F^{(2)} = \tfrac{T^2}{96}\Big(\Big[\widehat{B},\, [\widehat{B}, \widehat{A}]\Big] + \Big[\widehat{A},\, [\widehat{A}, \widehat{B}]\Big]\Big),$$

$$\widehat{H}_F^{(3)} = -\,\tfrac{T^3}{284}\Big[\widehat{A},\, [\widehat{B},\, [\widehat{B}, \widehat{A}]]\Big].$$

By formally replacing the quantum commutator $[\cdot,\cdot]$ with the classical Poisson bracket $\{\cdot,\cdot\}$, the Magnus expansion carries over to classical spins. Up to third order in the period T, one obtains

$$H_F^{(0)} = \tfrac{1}{2}\sum_{j=1}^{N}\Big(J\,S_j^z S_{j+1}^z + h\,S_j^z + g\,S_j^x\Big),$$

$$H_F^{(1)} = -\frac{g\,T}{8}\sum_{j=1}^{N}\Big[J\,(S_{j+1}^z + S_{j-1}^z) + h\Big]\,S_j^y,$$

$$H_F^{(2)} = \frac{T^2}{96}\sum_{j=1}^{N}\Big[J\,g^2\Big(S_j^y\,(S_{j+1}^y + S_{j-1}^y) - S_k^z\,(S_{j+1}^z + S_{j-1}^z)\Big) - g^2 h\,S_j^z$$
$$- 2Jg\,h\,(S_{j+1}^z + S_{j-1}^z)\,S_j^x - g\,h^2\,S_j^x - J^2 g\Big(2S_{j+1}^z S_{j-1}^z + (S_{j+1}^z)^2 + (S_{j-1}^z)^2\Big)\Big],$$

$$H_F^{(3)} = \frac{T^3}{284}\sum_{j=1}^{N}\Big[J\,g^2\,h\,S_j^x\,(S_{j+1}^z + S_{j-1}^z) + J^2 g^2\,S_j^z\,S_{j+1}^x\,(S_{j+1}^z + S_{j-1}^z) + J^2 g^2\,S_j^z\,S_{j+2}^x\,(S_{j+2}^z + S_j^z)\Big].$$

1.2 Periodic Driving

In our classical spin chain the system is driven by alternating between two Hamiltonians:

$$H(t) = \begin{cases} H_1, & t \in [0, T/2) \mod T, \\ H_2, & t \in [T/2, T) \mod T, \end{cases}$$

where H_1 couples the z-components of neighboring spins and H_2 applies a transverse field along x. The drive frequency $\Omega = 2\pi/T$ sets a clear separation of timescales.

1.3 Heating and Thermalization

Generic many-body systems under periodic driving absorb energy until they thermalize to an infinite-temperature state, erasing any initial order. However, the heating rate Γ is exponentially suppressed in the drive frequency,

$$\Gamma \;\sim\; e^{-c\,\Omega/J},$$

for some constant $c > 0$. One tracks the normalized excess energy

$$\langle Q(lT)\rangle = \frac{\langle H_F\rangle_{lT} - E_{\mathrm{GS}}}{\langle H_F\rangle_{\beta=0} - E_{\mathrm{GS}}},$$

which varies between 0 (no absorption) and 1 (full thermalization) and only reaches unity after an exponentially large number of cycles $l_{\mathrm{th}} \sim e^{\gamma\,\Omega}$. Here E_{GS} is the ground-state energy of the infinite-frequency Hamiltonian $H_F^{(0)}$, and $\langle\cdot\rangle_{\beta=0}$ denotes the infinite-temperature average.

1.4 Prethermalization

Before true thermalization, the system relaxes rapidly into a long-lived quasi-steady "prethermal plateau" governed by the effective Hamiltonian H_F up to a given expansion order. During this plateau (for $l \ll l_{\text{th}}$), observables such as the staggered magnetization

$$M^{\alpha}(lT) = \frac{1}{N}\sum_{j}(-1)^{j} S_j^{\alpha}(lT)$$

remain close to their ground-state values of H_F, with only small fluctuations. This prethermal regime thus provides a window to observe and manipulate Floquet-engineered phases in experiment, provided the drive frequency is sufficiently high to delay heating.

Chapter 2

Model

We Consider a classical Ising chain with periodic boundary conditions, described by the energy function

$$H(t) = \begin{cases} \sum_{j=1}^{N} \left(J\, S_j^z S_{j+1}^z + h\, S_j^z \right), & t \in \left[0, \frac{T}{2}\right) \mod T, \\ \sum_{j=1}^{N} g\, S_j^x, & t \in \left[\frac{T}{2}, T\right) \mod T. \end{cases} \tag{2.1}$$

Here, J denotes the nearest-neighbor interaction strength, while h and g are the magnetic field strengths along the z and x directions, respectively.

The spin (or rotor) variable $\vec{S}_j$, with $\|\vec{S}_j\| = 1$, on site j satisfies the Poisson bracket relation

$$\{S_i^\mu, S_j^\nu\} = \delta_{ij}\, \epsilon^{\mu\nu\rho}\, S_j^\rho, \tag{2.2}$$

where $\epsilon^{\mu\nu\rho}$ is the fully antisymmetric tensor.

The time dependence arises due to the periodic switching between two time-independent Hamiltonians, each acting for a duration of $T/2$ with frequency

$$\Omega = \frac{2\pi}{T}. \tag{2.3}$$

The time evolution of the system is governed by Hamilton's equations of motion,

$$\frac{dS_j^\mu(t)}{dt} = \{S_j^\mu, H(t)\}. \tag{2.4}$$

Chapter 3

Equations of motion

The system is driven by switching between two different time-independent Hamiltonians. For a total period T, one uses:

- **First half** $\left(t \in \left[0, \frac{T}{2}\right)\right)$**:** The Hamiltonian H_1 depends only on the z-components (and interactions between them).
- **Second half** $\left(t \in \left[\frac{T}{2}, T\right)\right)$**:** The Hamiltonian H_2 depends only on the x-components.

In particular, for the spin components we have

$$\frac{dS_j^\mu}{dt} = \{S_j^\mu, H\} = \sum_\nu \frac{\partial H}{\partial S_j^\nu}\{S_j^\mu, S_j^\nu\}, \tag{3.1}$$

and using the Poisson bracket relation

$$\{S_j^\mu, S_j^\nu\} = \epsilon^{\mu\nu\rho}\, S_j^\rho, \tag{3.2}$$

we can write

$$\frac{dS_j^\mu}{dt} = \sum_\nu \frac{\partial H}{\partial S_j^\nu}\, \epsilon^{\mu\nu\rho}\, S_j^\rho. \tag{3.3}$$

This formula will be applied for each half of the driving period.

3.1 First Half-Period: Rotation About the z-Axis (Map τ_1)

During the first half-period $t \in \left[0, \frac{T}{2}\right)$, the Hamiltonian is

$$H_1 = \sum_{j=1}^{N} \left(J\, S_j^z S_{j+1}^z + h\, S_j^z\right). \tag{3.4}$$

Notice that H_1 depends only on S^z. For a given spin j,

$$\frac{\partial H_1}{\partial S_j^z} = J\Big(S_{j-1}^z + S_{j+1}^z\Big) + h \equiv \kappa_j, \tag{3.5}$$

and

$$\frac{\partial H_1}{\partial S_j^x} = \frac{\partial H_1}{\partial S_j^y} = 0. \tag{3.6}$$

Using the general formula for Hamilton's equations of motion,

$$\frac{dS_j^\mu}{dt} = \sum_\nu \frac{\partial H_1}{\partial S_j^\nu}\, \epsilon^{\mu\nu\rho}\, S_j^\rho, \tag{3.7}$$

only the term with $\nu = z$ contributes since H_1 depends solely on S^z. Thus,

$$\frac{dS_j^\mu}{dt} = \frac{\partial H_1}{\partial S_j^z}\, \epsilon^{\mu z\rho}\, S_j^\rho = \kappa_j\, \epsilon^{\mu z\rho}\, S_j^\rho. \tag{3.8}$$

Now, writing this out component by component:

For $\mu = x$: The only nonzero component is for $\rho = y$ (since $\epsilon^{xzy} = -1$), so

$$\frac{dS_j^x}{dt} = -\kappa_j\, S_j^y. \tag{3.9}$$

For $\mu = y$: The nonzero contribution is for $\rho = x$ (with $\epsilon^{yzx} = +1$), hence,

$$\frac{dS_j^y}{dt} = \kappa_j\, S_j^x. \tag{3.10}$$

For $\mu = z$: Since $\epsilon^{zz\rho} = 0$ for any ρ, we obtain

$$\frac{dS_j^z}{dt} = 0. \tag{3.11}$$

These equations describe a rotation in the xy-plane about the z-axis by an angle $\theta = \kappa_j \frac{T}{2}$.

3.2 Second Half-Period: Rotation About the x-Axis (Map τ_2)

During the second half-period $t \in \left[\frac{T}{2}, T\right)$, the Hamiltonian is

$$H_2 = \sum_{j=1}^{N} g\, S_j^x. \tag{3.12}$$

Here, the Hamiltonian depends only on S^x. For a given spin j,

$$\frac{\partial H_2}{\partial S_j^x} = g, \tag{3.13}$$

and

$$\frac{\partial H_2}{\partial S_j^y} = \frac{\partial H_2}{\partial S_j^z} = 0. \tag{3.14}$$

Again, using the general formula,

$$\frac{dS_j^\mu}{dt} = \sum_\nu \frac{\partial H_2}{\partial S_j^\nu}\, \epsilon^{\mu\nu\rho}\, S_j^\rho, \tag{3.15}$$

only the term with $\nu = x$ contributes:

$$\frac{dS_j^\mu}{dt} = \frac{\partial H_2}{\partial S_j^x}\, \epsilon^{\mu x\rho}\, S_j^\rho = g\, \epsilon^{\mu x\rho}\, S_j^\rho. \tag{3.16}$$

Now, writing this out component by component:

- For $\mu = y$:

  The only nonzero contribution is for $\rho = z$ (since $\epsilon^{yxz} = -1$), so

$$\frac{dS_j^y}{dt} = -g\, S_j^z. \tag{3.17}$$

- For $\mu = z$: The nonzero contribution is for $\rho = y$ (with $\epsilon^{zxy} = +1$), hence,

$$\frac{dS_j^z}{dt} = g\, S_j^y. \tag{3.18}$$

- For $\mu = x$: Since $\epsilon^{xx\rho} = 0$ for any ρ, we have

$$\frac{dS_j^x}{dt} = 0. \tag{3.19}$$

These equations describe a rotation in the yz-plane about the x-axis by an angle $\theta = g\,\frac{T}{2}$.

3.3 Summary of evolution over the entire period

First Half-Period (τ_1): The spins rotate in the xy-plane about the z-axis with a spin-dependent rotation angle $\kappa_j\,\frac{T}{2}$. This yields:

$$S_j^x\left(\frac{T}{2}\right) = S_j^x(0)\cos\left(\kappa_j\,\frac{T}{2}\right) - S_j^y(0)\sin\left(\kappa_j\,\frac{T}{2}\right), \tag{3.20}$$

$$S_j^y\left(\frac{T}{2}\right) = S_j^x(0)\sin\left(\kappa_j\,\frac{T}{2}\right) + S_j^y(0)\cos\left(\kappa_j\,\frac{T}{2}\right), \tag{3.21}$$

$$S_j^z\left(\frac{T}{2}\right) = S_j^z(0). \tag{3.22}$$

Second Half-Period (τ_2): The spins then rotate in the yz-plane about the x-axis with an angle $g\,\frac{T}{2}$:

$$S_j^y(T) = S_j^y\left(\frac{T}{2}\right)\cos\left(g\,\frac{T}{2}\right) - S_j^z\left(\frac{T}{2}\right)\sin\left(g\,\frac{T}{2}\right), \tag{3.23}$$

$$S_j^z(T) = S_j^y\left(\frac{T}{2}\right)\sin\left(g\,\frac{T}{2}\right) + S_j^z\left(\frac{T}{2}\right)\cos\left(g\,\frac{T}{2}\right), \tag{3.24}$$

$$S_j^x(T) = S_j^x\left(\frac{T}{2}\right). \tag{3.25}$$

Chapter 4

Modified Hamiltonian

In this study, we will also include a modified Hamiltonian. Instead of the linear $h\,S_j^z$ term, consider a quadratic term $\alpha\,(S_j^z)^2$.
New Hamiltonian: For $0 \le t < T/2$,

$$H_1 \;=\; \sum_{j=1}^{N}\Big(J\,S_j^z S_{j+1}^z \;+\; h\,(S_j^z)^2\Big),$$

and for $T/2 \le t < T$,

$$H_2 \;=\; \sum_{j=1}^{N} g\,S_j^x.$$

The $h\,(S_j^z)^2$ term modifies the local spin potential, potentially altering the prethermal plateau duration and the ultimate heating dynamics. We will investigate whether the system still exhibits a long-lived prethermal state and how synchronization or heating transition times are affected.

4.1 Equations of Motion for the Modified Hamiltonian

As before, we switch between

$$H(t) = \begin{cases} H_1 = \displaystyle\sum_{j=1}^{N}\Big(J\,S_j^z S_{j+1}^z + h\,(S_j^z)^2\Big), & t \in [0, T/2) \bmod T, \\ H_2 = \displaystyle\sum_{j=1}^{N} g\,S_j^x, & t \in [T/2, T) \bmod T. \end{cases}$$

The general Poisson-bracket form is

$$\frac{dS_j^\mu}{dt} \;=\; \{\,S_j^\mu,\; H\,\} \;=\; \sum_\nu \frac{\partial H}{\partial S_j^\nu}\,\epsilon^{\mu\nu\rho}\,S_j^\rho.$$

4.1.1 First Half–Period: Rotation about z-Axis

Here $H = H_1$. Nonzero derivatives are

$$\frac{\partial H_1}{\partial S_j^z} = J\,(S_{j-1}^z + S_{j+1}^z) + 2h\,S_j^z, \qquad \frac{\partial H_1}{\partial S_j^x} = \frac{\partial H_1}{\partial S_j^y} = 0.$$

Thus

$$\frac{dS_j^\mu}{dt} = \Big[J\,(S_{j-1}^z + S_{j+1}^z) + 2h\,S_j^z\Big]\,\epsilon^{\mu z\rho}\,S_j^\rho.$$

Writing out components,

$$\frac{dS_j^x}{dt} = -\Big[J\,(S_{j-1}^z + S_{j+1}^z) + 2h\,S_j^z\Big]\,S_j^y, \tag{4.1}$$

$$\frac{dS_j^y}{dt} = \Big[J\,(S_{j-1}^z + S_{j+1}^z) + 2h\,S_j^z\Big]\,S_j^x, \tag{4.2}$$

$$\frac{dS_j^z}{dt} = 0. \tag{4.3}$$

4.1.2 Second Half–Period: Rotation about x-Axis

Here $H = H_2$. Nonzero derivative:

$$\frac{\partial H_2}{\partial S_j^x} = g, \qquad \frac{\partial H_2}{\partial S_j^y} = \frac{\partial H_2}{\partial S_j^z} = 0.$$

Hence

$$\frac{dS_j^\mu}{dt} = g\,\epsilon^{\mu x\rho}\,S_j^\rho,$$

or componentwise,

$$\frac{dS_j^y}{dt} = -\,g\,S_j^z, \tag{4.4}$$

$$\frac{dS_j^z}{dt} = \,g\,S_j^y, \tag{4.5}$$

$$\frac{dS_j^x}{dt} = 0. \tag{4.6}$$

4.1.3 Summary of Evolution over One Full Cycle

Denote the maps for each half-period by τ_1 (rotation about z) and τ_2 (rotation about x). Starting from $\mathbf{S}_j(0)$:

After τ_1 (time $T/2$):

$$\begin{aligned}
S_j^x\Big(\tfrac{T}{2}\Big) &= S_j^x(0)\,\cos\Big(\kappa_j\,\tfrac{T}{2}\Big) - S_j^y(0)\,\sin\Big(\kappa_j\,\tfrac{T}{2}\Big),\\
S_j^y\Big(\tfrac{T}{2}\Big) &= S_j^x(0)\,\sin\Big(\kappa_j\,\tfrac{T}{2}\Big) + S_j^y(0)\,\cos\Big(\kappa_j\,\tfrac{T}{2}\Big),\\
S_j^z\Big(\tfrac{T}{2}\Big) &= S_j^z(0),
\end{aligned}$$

where $\kappa_j = J\,(S_{j-1}^z + S_{j+1}^z) + 2h\,S_j^z$.

After τ_2 (time T):

$$\begin{aligned}
S_j^y(T) &= S_j^y\Big(\tfrac{T}{2}\Big)\cos\Big(g\,\tfrac{T}{2}\Big) - S_j^z\Big(\tfrac{T}{2}\Big)\sin\Big(g\,\tfrac{T}{2}\Big),\\
S_j^z(T) &= S_j^y\Big(\tfrac{T}{2}\Big)\sin\Big(g\,\tfrac{T}{2}\Big) + S_j^z\Big(\tfrac{T}{2}\Big)\cos\Big(g\,\tfrac{T}{2}\Big),\\
S_j^x(T) &= S_j^x\Big(\tfrac{T}{2}\Big).
\end{aligned}$$

Thus the full-cycle map is $\mathbf{S}_j(T) = \tau_2 \circ \tau_1\Big[\mathbf{S}_j(0)\Big]$.

Chapter 5

Methodology

5.1 Ground-State Preparation at High Drive Frequencies

5.1.1 Linear Hamiltonian

Time-Averaged Hamiltonian $H_{\mathbf{ave}}$ We prepare the system at $t = 0$ in the ground state of the *time-averaged* Hamiltonian:

$$H_{\text{ave}} \;=\; \frac{1}{2}\sum_{j=1}^{N}\Big(J\,S_j^z\,S_{j+1}^z \;+\; h\,S_j^z \;+\; g\,S_j^x\Big).$$

Energy Density and AFM Order

- For parameters $g/J = 0.9045$ and $h/J = 0.809$, the ground state of H_{ave} has an energy density $E_{\text{GS}}/N \approx -1.235\,J$.
- Whenever J, h, and g share the same sign and are of similar magnitude, the ground state exhibits **antiferromagnetic (AFM) order** in the xz-plane.
- Translational invariance allows the ground-state evolution to be effectively described by two coupled spin degrees of freedom (an AFM unit cell).

5.1.2 Quadratic Hamiltonian

Time-Averaged Hamiltonian H_{ave}: At $m = 0$, the time-averaged Hamiltonian with the quadratic tweak is

$$H_{\text{ave}} = \frac{1}{2}\sum_{j=1}^{N}\Big(J\,S_j^z S_{j+1}^z \;+\; h\,(S_j^z)^2 \;+\; g\,S_j^x\Big)\,.$$

Energy Density and Stationary Conditions: By translational invariance[2] and absence of any y-field, we compare:

1. **Uniform tilt**

$$\vec{S}_j = (\sin\theta,\, 0,\, \cos\theta),$$

giving

$$E_{\text{uni}}(\theta) = \frac{1}{2}\Big[(J+\alpha)\cos^2\theta + g\,\sin\theta\Big].$$

Differentiating w.r.t. θ:

$$\frac{dE_{\text{uni}}}{d\theta} = \frac{1}{2}\Big[-2(J+\alpha)\cos\theta\sin\theta + g\cos\theta\Big] = 0 \implies (J+\alpha)\tan\theta = \frac{g}{2},$$

so the optimal uniform tilt satisfies $\sin\theta = \frac{g}{2(J+\alpha)}$ (or $\theta = 90^\circ$ if that ratio exceeds 1).

2. **Canted AFM order**

$$\vec{S}_{2k} = (\sin\theta, 0, \cos\theta), \quad \vec{S}_{2k+1} = (\sin\theta, 0, -\cos\theta),$$

giving

$$E_{\text{AF}}(\theta) = \frac{1}{2}\Big[(\alpha - J)\cos^2\theta + 2\,g\,\sin\theta\Big].$$

Differentiating,

$$\frac{dE_{\text{AF}}}{d\theta} = \frac{1}{2}\Big[-2(\alpha-J)\cos\theta\sin\theta + 2g\cos\theta\Big] = 0 \implies (\alpha - J)\tan\theta = g,$$

so the optimal AFM canting satisfies $\sin\theta = \frac{g}{(\alpha - J)}$ (or $\theta = 90^\circ$ if out of bounds).

Choosing the Ground State We compute $E_{\text{uni}}(\theta_{\text{uni}})$ and $E_{\text{AF}}(\theta_{\text{AF}})$, then initialize the chain in the configuration (uniform or two-sublattice AFM) whose energy is lower.

5.2 Noise Realizations and Ensemble Averages

This is same for both the Hamiltonians.

Small Random Perturbations

- To allow the system to thermalize (breaking perfect translational symmetry), we add *small random noise* to each spin's orientation.
- Each spin's azimuthal angle is perturbed by a random value in $[-\pi/100,\ \pi/100]$.
- This noise ensures that the chain is not stuck in a perfectly ordered configuration.

Ensemble Averages and Independence from Noise Strength

- All observables are averaged over an ensemble of 20 noisy initial-state realizations.
- Long-time dynamics remain **independent of the exact noise strength**, provided the noise is small enough not to alter the system's total energy significantly.
- We denote ensemble-averaged quantities by $\langle\cdot\rangle$.

5.2.1 Four Dynamical Stages of Evolution

These are the expected stages of evolution for the linear Hamiltonian case. Real Simulation may differ for the quadratic case.

- **Initial Transient:** Rapid, partial thermalization from the ordered initial state. Local degrees of freedom absorb energy until constrained by short-range correlations, and the mean energy quickly saturates to a finite value.

- **Prethermal Plateau:** A long-lived quasi-equilibrium regime in which energy absorption stalls exponentially in the driving frequency Ω. The system behaves as if thermalized with respect to an effective Floquet Hamiltonian H_F obtained from an inverse-frequency expansion.
- **Late Crossover:** The breakdown of approximate conservation laws (via rare many-body resonances) leads to a rapid increase in energy absorption and in the variance of local observables, marking the end of the prethermal plateau.
- **Infinite-Temperature Steady State:** At very long times, the system reaches a featureless, maximum-entropy state. Local variables are completely randomized, and all observables take their infinite-temperature values.

Note: The heating time (the time at which energy fluctuations peak) grows exponentially with the drive frequency.

5.3 Energy Observables: $\langle Q(lT)\rangle$

Expected Energy $\langle Q(lT)\rangle$ Defined as the normalized excess energy:

$$\langle Q(lT)\rangle \;=\; \frac{\langle H_{\text{ave}}[\{\mathbf{S}_j(lT)\}]\rangle - E_{\text{GS}}}{\langle H_{\text{ave}}\rangle_{\beta=0} - E_{\text{GS}}},$$

where:

- H_{ave} is the time-averaged (infinite-frequency) Hamiltonian.
- E_{GS} is the ground state energy.
- $\langle H_{\text{ave}}\rangle_{\beta=0}$ is the energy expectation in an infinite-temperature ensemble.

Thus, $\langle Q(lT)\rangle = 0$ means no energy is absorbed, while $\langle Q(lT)\rangle = 1$ corresponds to full thermalization.

5.4 Noise-Averaged Expected Energy vs. Driving Cycles

This is the graph given in for the linear hamiltonian which shows all the four stages of the evolution[1].

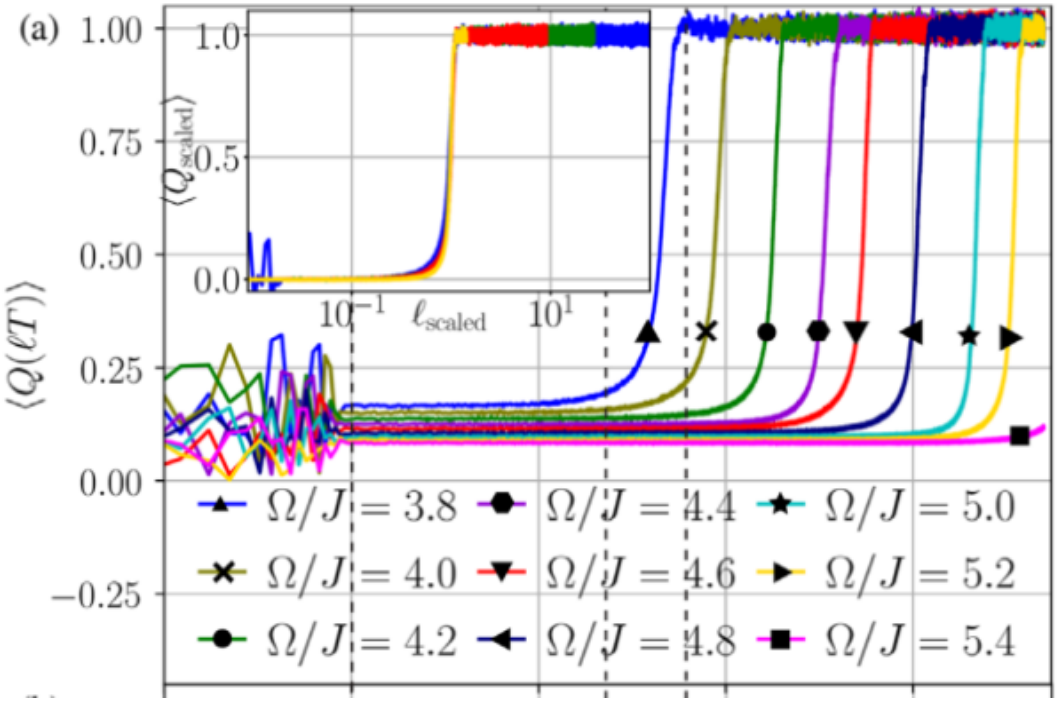

Figure 5.1: Graph of Noise-Averaged Expected Energy vs. Driving Cycles

Chapter 6

Simulation and Code

We decided to simulate this system in C++ as we found it to be much faster than Python.

6.1 Explanation of the C++ Simulation Code for the Linear Hamiltonian

1. Overall Simulation Flow

- **Data structures and parameters:**
  - `using Spins = std::vector<std::array<double,3>>;` a chain of N spins, each (S_x, S_y, S_z).
  - Physical constants: J, h, g (couplings/fields), Ω (drive frequency), $T = 2\pi/\Omega$, θ (initial tilt), *noise_amp*.
- **`initialize_spins`:**
  - Samples (S_x, S_y) uniformly in a small disk of radius $\delta_{\text{ini}} = 0.1$.
  - Sets $S_z = \pm\sqrt{1 - S_x^2 - S_y^2}$ in an alternating pattern.
- **`compute_H_ave`:**

$$H \;=\; \sum_{j=0}^{N-1} \Big(J\, S_j^z S_{j+1}^z + h\, S_j^z + g\, S_j^x \Big), \quad E = \tfrac{1}{2}\, H$$

  Computes and returns the half-chain energy to avoid double-counting.
- **`update_spins`:** one Floquet cycle
  1. Build local mean fields $\kappa_j = J\,(S_{j-1}^z + S_{j+1}^z) + h$.
  2. For each spin:
     - Rotate about z by $\phi_j = \frac{1}{2}\,\kappa_j\, T$.
     - Rotate about x by $\theta_x = \frac{1}{2}\, g\, T$.
- **`simulate_run`:**
  - Initializes a fresh random spin chain.

- Performs L update cycles, recording H after each.
- Returns vector $\{Q(0), Q(1), \ldots, Q(L)\}$.

- **`ensemble_average`:**
  - Launches *num_runs* independent simulations (see below).
  - Averages their outputs and normalizes $Q_{\text{avg}}(\ell) \leftarrow \dfrac{Q_{\text{avg}}(\ell) - E_0}{-E_0}$.

- **I/O and plotting:**
  - Write $\{Q_{\text{avg}}\}$ to `results.txt`.
  - Generate a small Gnuplot script `plot.gp` and invoke `std::system("gnuplot plot.gp")`.

2. Parallelism via

```
// Launch each run in its own background task
std::vector<std::future<std::vector<double>>> futures;
for (int run = 0; run < num_runs; ++run) {
    unsigned int seed = std::random_device{}() + run;
    futures.push_back(
        std::async(std::launch::async,
                   simulate_run,
                   L, N, J, h, g, T, theta, noise_amp, seed)
    );
}

// Collect results once ready
std::vector<double> Q_ensemble(L+1, 0.0);
for (int run = 0; run < num_runs; ++run) {
    auto Q_run = futures[run].get();  // blocks until simulation
       finishes
    for (int l = 0; l <= L; ++l) {
        Q_ensemble[l] += Q_run[l];
    }
}
```

- **`std::async(std::launch::async, ...)`** Immediately launches each call to `simulate_run` in a new thread (or thread-pool), returning a `std::future`.
- **`future.get()`** Blocks until that particular simulation completes, then returns its data.
- Each spin chain simulation is independent.

This program simulates a periodically driven 1D spin chain under Floquet dynamics, measures its energy absorption over many cycles, and uses C++11 `std::async` + `std::future` to perform an ensemble average in parallel.

6.2 Explanation of the C++ Simulation Code for the Quadratic Hamiltonian

We now describe the numerical protocol used to study heating in the spin chain with the quadratic tweak. The procedure is almost identical except for the Ground state iinitialization and average normalized excess energy calculation. The Hamiltonian is

$$H(t) = \begin{cases} \sum_{j=1}^{N} \Big(J\, S_j^z S_{j+1}^z \;+\; h\,(S_j^z)^2 \Big), & t \in [0, T/2) \bmod T, \\ \sum_{j=1}^{N} g\, S_j^x, & t \in [T/2, T) \bmod T, \end{cases}$$

and we track the average normalized excess energy

$$\Big\langle Q(lT) \Big\rangle = \frac{\Big\langle H_{\text{ave}}[\{\mathbf{S}_j(lT)\}] \Big\rangle - E_0}{\Big\langle H_{\text{ave}} \Big\rangle_{T\to\infty} - E_0},$$

where

$$H_{\text{ave}} = \frac{1}{2} \sum_{j=1}^{N} \Big(J\, S_j^z S_{j+1}^z + h\,(S_j^z)^2 + g\, S_j^x \Big)$$

is the period-0 effective Hamiltonian and E_0 its ground-state energy.

In the limit of infinitely long driving time ($T \to \infty$, or equivalently $l \to \infty$), the system reaches the infinite-temperature steady state and all spin orientations become equally likely on the unit sphere. Hence

$$\Big\langle S_j^x \Big\rangle_{T\to\infty} = \Big\langle S_j^z \Big\rangle_{T\to\infty} = 0, \quad \Big\langle \big(S_j^z\big)^2 \Big\rangle_{T\to\infty} = \frac{1}{3}.$$

For the quadratic Hamiltonian

$$H_{\text{ave}} = \frac{1}{2} \sum_{j=1}^{N} \Big(J\, S_j^z S_{j+1}^z + h\,(S_j^z)^2 + g\, S_j^x \Big),$$

we then have

$$\Big\langle S_j^z S_{j+1}^z \Big\rangle_{T\to\infty} = \Big\langle S_j^z \Big\rangle_{T\to\infty} \Big\langle S_{j+1}^z \Big\rangle_{T\to\infty} = 0,$$

and therefore

$$\Big\langle H_{\text{ave}} \Big\rangle_{T\to\infty} = \frac{1}{2} \sum_{j=1}^{N} \Big(J \cdot 0 + h \cdot \tfrac{1}{3} + g \cdot 0 \Big) = \frac{N}{2}\, \frac{h}{3} = \frac{N\,h}{6}.$$

Hence the infinite-time, per-spin energy is

$$\lim_{T\to\infty} \frac{1}{N} \Big\langle H_{\text{ave}} \Big\rangle = \frac{h}{6}.$$

Ground-State Initialization We compare two variational tilts θ in the xz plane:

$$\theta_{\text{uni}}\colon \quad \vec{S}_j = (\sin\theta, 0, \cos\theta), \qquad E_{\text{uni}}(\theta) = \tfrac{1}{2}\Big[(J+h)\cos^2\theta + g\sin\theta\Big],$$

$$\theta_{\text{AF}}\colon \quad \vec{S}_{2k} = (\sin\theta, 0, \cos\theta),\ \vec{S}_{2k+1} = (\sin\theta, 0, -\cos\theta), \quad E_{\text{AF}}(\theta) = \tfrac{1}{2}\Big[(h-J)\cos^2\theta + 2g\sin\theta\Big].$$

We find each optimal θ by solving $\frac{dE}{d\theta} = 0$, i.e. $(J+h)\tan\theta = \frac{g}{2}$ or $(h-J)\tan\theta = g$, respectively, (and cap $\theta = 90°$ if $\sin\theta > 1$), then choose the lower-energy ansatz.[1]

[1] The code used for the simulations is available on GitHub[3]

Chapter 7

Results and Discussion

7.1 Linear Hamiltonian Results

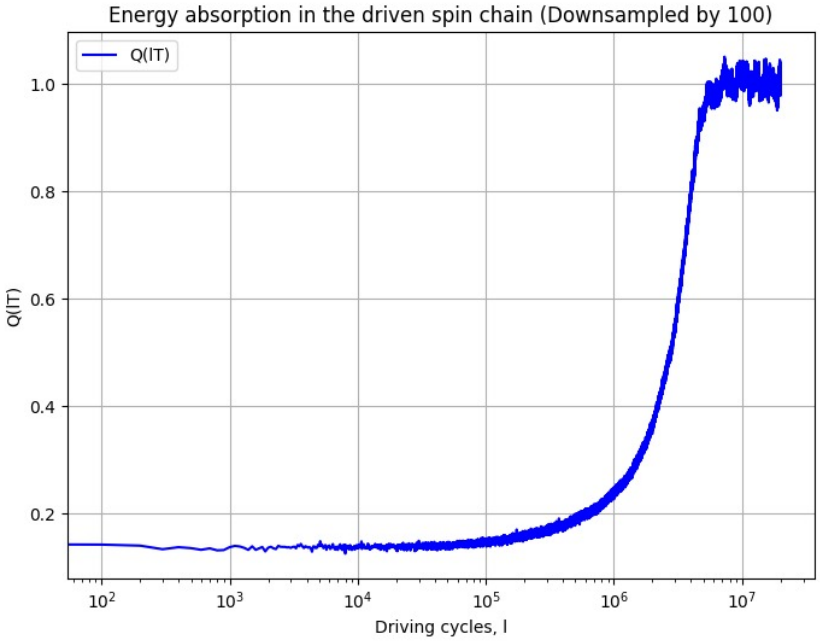

- The figure shows the noise-averaged expected energy versus driving cycles for $\Omega/J = 3.8$.
- The simulation demonstrates a long-lived prethermal plateau before rapid heating.

7.2 Quadratic Hamiltonian Results

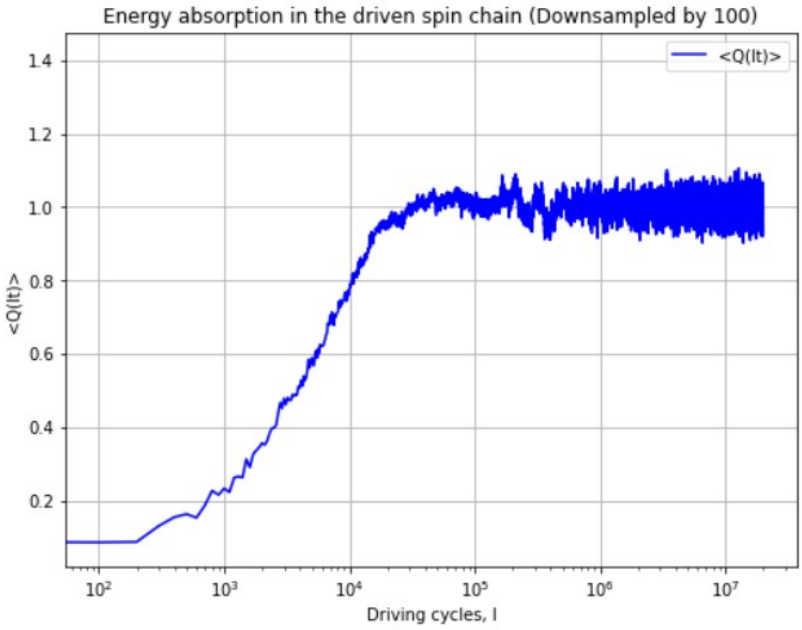

- The figure shows the noise-averaged expected energy versus driving cycles for $\Omega/J = 3.8$.
- The simulation demonstrates gradual heating to infinite temperature without any prethermal plateau for this value of Ω.

Chapter 8

Scope for Advancement

A worthwhile extension of the current research is to use *block mutual information* (BMI) as a probe of the dynamical heating transition. BMI quantifies the total correlations between two consecutive segments of the spin chain and can be formulated classically or quantum-mechanically as

$$I(A{:}B) = S(A) + S(B) - S(A \cup B),$$

where $S(X)$ is the Shannon entropy of the marginal distribution on block X, or the von Neumann entropy of the reduced density matrix ρ_X.

8.1 Expected Behavior During Thermalization

1. **Prethermal plateau:** Spins initialized in a canted AFM pattern exhibit only short-range correlations, so $I(A{:}B)$ remains low and approximately constant.

2. **Late crossover (heating onset):** As the drive injects energy, correlations spread across the chain. BMI grows from its plateau value, rising sharply.

3. **Peak correlations:** At the heating time $l_{\max}$, $I(A:B)$ attains a pronounced maximum, reflecting maximal shared information between blocks.

4. **Infinite-temperature steady state:** The system approaches a fully random ensemble; distant blocks decouple, and $I(A{:}B)$ decays back toward zero.

This BMI-based work will reveal a number of important insights in addition to energy observables. The subsequent decay of I to zero defines the disappearance of all multi-spin correlations, representing the ultimate approach to infinite-temperature randomness. This will elucidate how correlations accumulate, peak, and decay in periodically driven many-body systems, and offer a more complete understanding of Floquet thermalization. We tried to do this but the process of this computation is exceptionally expensive and parallelization does not significantly reduce the computational time. The number of chain ensembles is on the order of 10000 or more in order to see any meaningful results.

Bibliography

[1] O. Howell, P. Weinberg, D. Sels, A. Polkovnikov, and M. Bukov, *Asymptotic Prethermalization in Periodically Driven Classical Spin Chains*, Phys. Rev. Lett. **122**, 010602 (2019). doi:10.1103/PhysRevLett.122.010602

[2] See Supplemental Material for *Analogy of the Physics of the Dynamical Heating Transition with the 1D Ising Model Close to Zero Temperature*, which provides additional discussion and derivations supporting the main text.

[3] A. Maheshwari, *Quantum Spin Thermalization Simulation Code*, GitHub repository: `https://github.com/anshulvvv/Quantum-Spin-Thermalization`